

Optimal, robust, and benign horizontal and vertical axis wind turbines

S P Farthing

Wing'd Pump Ltd, 975 Tuam Road, N. Saanich, British Columbia, Canada V8L 5P2. email: simon@econologica.com

The manuscript was received on 24 May 2006 and was accepted after revision for publication on 9 May 2007.

DOI: 10.1243/09576509JPE333

Abstract: The remarkable success of fixed speed and pitch 'propellers' in tapping the gusting and shifting wind begs explanation. Glauert's two-dimensional analysis of 'horizontal axis wind turbines' was an incomplete aside to aviation propeller theory in 1935, but is now the basis of most 'Hawt' algorithms. A very simple windmill optimum is found for his 'blade element momentum' theory, even for the movement inclined to the wind in 'vertical axis wind turbines'. Optimizing the two-dimensional 'Vawt' pitch cycles for high speed ratios matches the best Hawt power.

Making the optimum 'robust' to variation of the wind further discovers a Hawt blade element chord and fixed pitch with a very broad quartic optimum around the design wind and 'benign' avoidance of high aerodynamic load coefficients further from it; and finds a fixed cycle of pitching to give a benign quartic Vawt.

Keywords: blade element momentum theory, Hawt, Vawt, robust quartic optimum, trisection

1 INTRODUCTION

Froude idealized a propeller as a steady flow sieve-like 'actuator' where the momentum change tied the wake velocity deficit $2I$ to the rotor thrust and torque. Later Joukowski's two-dimensional aerofoil theory related the lift force of the rotor blade segments or 'elements' to their apparent wind ' W ', composed of the true wind T , their self wind $-S$ opposite to the blade velocity S , and the flow J induced by their lift, Fig. 1. Glauert [1] used the axisymmetry of the Hawt 'actuator' and ignored wake expansion to link $J = I$.

However, after so closing the model, Glauert could only awkwardly reverse-tabulate the independent speed ratio x of tangential speed S to windspeed T (against the optimum 'interference' a). After much algebra, the product of the blade solidity σ by its lift coefficient C_L emerged as just $4 - 4 \cos \varphi$, where φ is the apparent wind angle between W and S . Stewart [2] proposed choosing two values of a and optimal $\varphi(a)$ to separate the best σ and C_L .

That simple equation suggests the angle variables: φ and its $I = 0$ value $\xi = \cot^{-1} x$. This reformulation easily gives $\sigma C_L = 4 - 4 \cos \varphi$ via a new $\varphi = 2\xi/3$

solving Glauert's optimal Hawt. Then the blade (3/4 chord) angle of attack α is $\xi/3$ for Stewart's optimum as his two a values merge. This new trisection of the angle $\xi(x)$ between S and $T-S$ holds even for blades moving obliquely at any angle θ to the wind, allowing the first Hawt-consistent analysis of the Vawt.

2 VECTOR BEM EQUATION AND DIAGRAM

As in Fig. 1, consider a section of a continuum of minute blades of infinite aspect ratio with span unit vector ' k ' out of the page. For a Hawt (Fig. 1b), the axis of rotation at angular velocity Ω is a radius ' r ' beneath the page parallel to the true wind T . The 'egg-beater' Vawt axis is out of the page at a radius r in the unit direction n perpendicular to the blade path unit direction s .

Call the velocity change the blades produce downstream ' $2I$ '. Then oppose the aerofoil lift ' dL ' by the net blade element chord, σds , to the rate of change of momentum of the flux $(T + J) \cdot n ds = W \cdot n ds$ of fluid density ' ρ ' passing through ' $s ds$ ', a minute increment

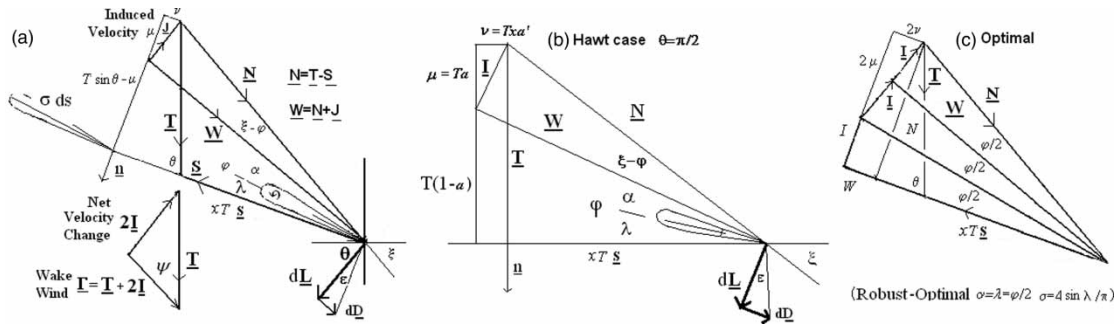


Fig. 1 Nominal and apparent winds (a) general, (b) Hawt case $\theta = \pi/2$, and (c) optimal

of the path (and ignore any net pressure force on the stream tube walls and ends).

$$\frac{1}{2} \rho W C_L k \times W \sigma ds = -dL = 2\rho I(W \cdot n) ds$$

(the blade element momentum (BEM) equation) (1)

Appendix 2 examines the basis and generality of the standard Hawt $J = I$ used next to find a simple exact solution of the optimal windmill actuator.

3 SIMPLE EXACT SOLUTION OF THE OPTIMAL WINDMILL ACTUATOR

Add the true wind T and the self-wind $-S = -xT$ spanning angle θ , to get the undisturbed No-lift, Nominal, or Naive apparent wind $N = T - S$ at angle ξ to S . Then to form the real total blade apparent wind W at angle φ , the induced velocity J , given in Appendix 2 as I and perpendicular to W as in equation (1) must be added to N , as in Fig. 1. The power P is blade velocity times thrust, so from equation (1)

$$\frac{dP}{ds} = 2\rho xTv(W \cdot n) \tag{2}$$

with $v = I \sin \varphi, I = N \sin(\xi - \varphi), W \cdot n = W \sin \varphi, W = N \cos(\xi - \varphi),$

$$\frac{dP}{ds} = \rho xTN^2 \sin^2 \varphi \sin 2(\xi - \varphi) \tag{3}$$

Defining the Vawt normal interference $a = I \cdot n/T \cdot n = \mu/T \sin \theta \rightarrow 1 - \varphi/\xi$ generalizes Glauert's equation (2.4) as the $m = 1/x \rightarrow 0$ and $\xi \rightarrow m \sin \theta$ limit of equation (3)

$$\frac{dP}{ds} \rightarrow 2\rho(T \cdot n)^3 (1 - a)^2 a + O(m \cos \theta, ma) \tag{4}$$

The $T \cdot n$ generalizes $T \sin \theta$ to discard any spanwise component of T in the Darrieus 'catenary' Vawt and shows the best Hawt power to asymptote as the cube of the cosine of any yaw.

The φ derivative of dP/ds in equation (3) is $2\rho xTN^2 \sin \varphi \sin(2\xi - 3\varphi)$ vanishing at the best

$$\varphi = \frac{2\xi}{3} \tag{5}$$

Hence the optimum angular interference $1 - \varphi/\xi$ is $1/3$ at all x and θ that have $J = I$.

Reflecting N about W as in Fig. 1(c) then shows optimally

$$T \sin \theta = I + 2\mu = \mu(2 + 1/\cos \varphi) \tag{6}$$

In terms of Glauert's key $a = \mu/T \sin \theta$

$$\cos \varphi = \frac{a}{(1 - 2a)} \tag{7}$$

Then the wake/actuator area $= (1 - a)/(1 - 2a) = 1 + \cos \varphi$, and now

$$xa' = v/T \sin \theta = \frac{\sin \varphi}{(1 + 2 \cos \varphi)} \tag{8}$$

Also by the reflection $W = W \cos \varphi + v$ and for $\theta = \pi/2, W = xT + 2v$ which discovers

$$a' = \frac{(1 - \cos \varphi)}{(2 \cos \varphi - 1)} \tag{9}$$

Proving Glauert's equation (2.19) and the identity

$$x = \cot\left(\frac{3\varphi}{2}\right) = \sin \varphi (2 \cos \varphi - 1) / (1 + 2 \cos \varphi)(1 - \cos \varphi) \tag{10}$$

From equation (3) at $\varphi = 2\xi/3$

$$\frac{dP}{ds} = \rho xTN^2 \sin^3 \varphi$$

$$\text{Then } d^2(dP/ds)/d^2\varphi = -6\rho xTN^2 \sin \varphi \tag{11}$$

Dividing the two gives a peak half width squared of $\sin^2 \varphi/6$ which compared with the scale φ^2 to the zeroes of dP/ds indicates a relatively sharper peak at large ξ , i.e. small x .

Alternatively for the Hawt case, a cubic in a [3] resulted from the substitution of Glauert's

equation (2.11) into his (2.12) with a solution based on the triple angle (cubic) sin identity which eventually could have been reduced to equations (5), (7), and (10) above.

4 ROBUSTLY OPTIMAL AND BENIGN BLADE ELEMENTS

Equation (1) and Fig. 1 give

$$\sigma C_L = 4 \sin \varphi \tan(\xi - \varphi) \tag{12}$$

Optimally $\xi - \varphi = \varphi/2$

$$\sigma C_L = 4 \sin \varphi \tan \varphi/2 = 4 - 4 \cos \varphi \tag{13}$$

If $\theta = \pi/2, k = \Omega c/T$

$$\begin{aligned} \sigma C_L x &= \frac{BkC_L}{2\pi} = 4(1 - \cos \varphi) \cot 3\varphi/2 \\ &= 4(2 \cos \varphi - 1) \sin \varphi / (2 \cos \varphi + 1) \end{aligned} \tag{14}$$

Glauert's equation (2.20) by trigonometric identity (10), which peaks at $\varphi = 35.5^\circ$ or $x \approx 3/4$.

At modest 3/4 chord angle of attack $\alpha, C_L/2\pi = \sin \alpha$, then equation (13) gives

$$\varpi \sin \alpha = \sin \varphi \tan \varphi/2 = 1 - \cos \varphi \tag{15}$$

if $\varpi = \pi\sigma/2 = Bc/4r$ for B blades each of chord c . As $m \downarrow 0$ non-optimal (12) linearizes to

$$\varpi \alpha \rightarrow (\xi - \varphi)\varphi \tag{16}$$

Glauert's 'indeterminacy' [1] between ϖ or σ , and α or C_L at the design ξ_d is easy to resolve optimally by requiring the rotor element fixed at 3/4 chord pitch angle $\lambda(r) = \varphi - \alpha$ and chord $c(r)$ to 'robustly' follow the optimal for a small change in $\xi(x, \theta)$ about ξ_d . For his optimal BEM equation (15) to continue to hold as φ then varies (as $2\xi/3$) is analogous to the stationarity of the similar terms in equation (3). By differentiation in $\varphi, \varpi \sin(\varphi - \lambda) = 1 - \cos \varphi$ despite φ varying at set ϖ and λ requires

$$\varpi \cos(\varphi - \lambda) = \sin \varphi \tag{17}$$

Dividing equations (15) by (17) gives $\tan \alpha = \tan 1/2\varphi$ so

$$\alpha = 1/2 \varphi = \lambda \tag{18}$$

completing the perfect exact optimal trisection of ξ_d into $\lambda, \alpha_d, \varphi_d/2$ with

$$\varpi = 2 \sin \alpha_d \uparrow \varphi_d \tag{19}$$

Thus the robust optimum angle λ of a blade element to its path is a third of the nominal design apparent wind angle ξ_d , and half the net apparent

wind angle φ_d . This pattern can now be recognised in Eggleston and Stoddard [4] tabulating Glauert's $a'(a), x(a', a), \varphi(x, a', a), \sigma C_L(\varphi)$ to get $\lambda = 7.7^\circ$ at mean $\alpha = 7.0^\circ \varphi_d = 14.7^\circ$ for a Hawt blade segment to be optimal at both $x = 2$ and 3 with mean $\xi_d = 21^\circ$.

To avoid the C_D of leading edge separation of small sheet metal blades, such thin circular arcs should be set like jibs to have no chordal angle of attack at ξ_d . To make this optimum robust, their trailing edges at twice the 3/4 chord α_d should be at φ_d , or just parallel to the motion.

For $\theta = \pi/2, Bk = 4x\varpi = 8 \sin(\xi/3)/\tan \xi \uparrow 8/3$ as $m \downarrow 0$. Thus the robustly optimum Hawt outer chord tends up to a constant $8T_d/3B\Omega_d$ [5], as Stewart [2] showed in the limit of his dual optimum points coalescing. His equation (22) implied $\alpha \approx 1/2\varphi$ but he did not recognize it or the following multitude of attributes.

Robust optimality allows Hawt performance to follow the optimal with small spatial variations in ξ over the blade path because of vertical gradients in wind speed, most significant for large wind turbines (especially large relative to their tower height). If gusts vary slowly in r/T , the time scale for passage through the rotor, the lift power everywhere stays optimum as the wind fluctuates in time, so especially for small windmills.

The robust condition gives the fixed blade operating coefficient of performance $C_p = 2(dP/ds)/\rho T^3$ a very broad kiss of the optimum C_p around the design ξ_d . With it $\varphi - 2\xi/3$ is zero and stationary in ξ at the design ξ_d and its Taylor series begins with the square of variations $\delta\xi$, negatively as seen from the feathering limit $\xi = \varphi = \lambda$. Since the expansion of C_p about its optimum for any ξ likewise begins with the square of $\varphi - 2\xi/3$, the combined expansion is a weak quartic $O(\delta\xi)^4$ whereas for non-robust blade angles and solidities it is a stronger quadratic decrease $O(\delta\xi)^2$, as illustrated in a followup analysis [6] and Fig. 2.

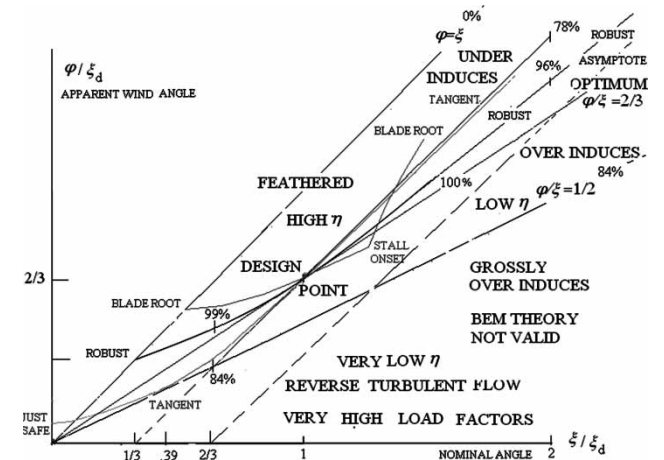


Fig. 2 φ versus ξ for four blade pitches with three φ/ξ zones

The robust off-peak $\varphi > 2\xi/3, a < 1/3$ benignly helps avoid high downwind induced drag $dE = 2\rho\{\mu(T \sin \theta - \mu)\}ds \rightarrow 2\rho(1 - a)a(T \sin \theta)^2 ds$ and structural loads away from the main power design point. Equation (32) shows the thrust efficiency $\eta = dP/T dE = \tan \varphi / \tan \xi$, is also the ratio of useful to total power removed from the stream and so an upper limit on array capture.

For $\theta = \pi/2$ and large x , compare tangent $\lambda = 0$ $\varpi = \kappa = \xi_d/3$ and $\alpha = \varphi = 2\kappa$ versus robust optimal $\varpi = 2\kappa$ and $\alpha = \lambda = \kappa$ element designs. For the tangent $\alpha = \varphi$ cancels in equation (16), reducing it to $\xi - \varphi = \varpi = \kappa$. Thus if ξ is doubled to 6κ , say by halving x , the tangent gets $\alpha = \varphi = 5\kappa$. However for the robust, equation (16) is quadratic yielding $\xi - \varphi = 1.55\kappa$, which ‘under-induces’ less versus the ideal $\varphi = 2\xi/3$. The C_p as $(1 - \varphi/\xi)(\varphi/\xi)^2$ equation (4) are reduced by 0.78 and 0.96, respectively, the loss ratio slightly exceeding the ratio of the above $(\varphi - 2\xi/3)^2$. Yet the difference in stall margin in favour of the robust $\varphi = 4.45\kappa$ has increased to $5\kappa - 3.45\kappa = 1.55\kappa$ from κ . Thus the tangent under-induces to exacerbate its higher design angle of attack for a much earlier stall. And if ξ is reduced to 2κ , robustly $a = 1 - \sqrt{1/2} = 0.29$ safely and slightly lower than optimal $1/3$ with C_p ratio 0.99, but for the tangent C_p ratio 0.84 at $a = 1/2$. This is the threshold of ‘turbulent’ [1] ‘over-induced’ reverse flow in the wake with heavy E at low C_p and so very low η .

The only price of the robust design is the higher profile drag penalty from the higher chord, but the followup will show it does not significantly shift the net optimum away from the robust for typical $\delta\xi$ from the wind and load regimes [6].

Figure 2 combines these results, with the robust operating curve kissing the high η side of the optimum $\varphi = 2\xi/3$ line at the design point.

Moving inwards on the Hawt blade $\alpha = \xi_d/3$ will reach a C_L peak at α_s later than static stall because of centrifugal stabilization of the boundary layer [7]. Then with C_L constant rather than linear, equation (12) gives $d\varphi/d\xi = 2/(2 - \cos \varphi) > 1$ so instead one needs a lesser $\alpha_d < \alpha_s$ to get the operating line closer on average to optimum, as labelled blade root in Fig. 2.

At the speed ratio for vanishing lift of approximately $3X_d$, T times the Hawt rotor net ‘drag’ equals the power lost to profile drag, approximately the integral of $1/2C_D(3Tx)^3 Bc dr$. For uniform (outer) robust chord, the rotor drag coefficient based on blade area and true wind is thus $C_D(3X_d)^3/4$ versus the drag coefficient of about 1 on the blade area if the rotor is locked against rotation. Since these are equal at low X_d of only 2.5 and freewheeling will have the greater drag moment arm and also large centrifugal forces, the robust optimal Hawt is not so benign as not to be better braked than freewheeled in very high winds.

5 APPLICATIONS TO FIXED PITCH HAWTS

Small blades are very strong for their weight and can furl to regulate or simply withstand the steady and productive loading of a near robust broad C_p peak, and they benefit most from its indifference to wind fluctuations of longer time scale than their small r/T . Raising the outer chord above the robust chord increases the zero rpm stalled blade torque for self starting. Whereas lower drag and chord blades more tangent than the robust may fatigue with the high rpm in unproductive turbulent over-inducing in high winds, as most off-grid loads are too weakly varying with Ω to prevent ξ decreasing with windspeed. At most their interference should kiss $1/2$, the threshold of reversed wake flow, at some $\xi_{1/2}$ below the design. The small angle BEM equation (16) $\varpi(\varphi - \lambda) = (\xi - \varphi)\varphi$ gives this minimum ‘just safe’ $\varpi = \xi_{1/2} = 0.39\xi_d$ with $\lambda = 0.29$ the robust. Such hyperbolae in Fig. 2 are asymptotic to the negative ξ axis.

Whereas grid-connected large Hawts can use synchronous generators to start and then to hold their rpm very constant. The robust advantage in off-design yawed running in windshifts is hard to quantify, though likely very significant with their active yaw power consumption. But their large size requires careful design not just for maximum annual power but also for minimum peak gravity and high wind blade bending moment. A near robust (tip) solidity produces too much absolute bending moment above the design wind, so the outer chord c , pitch λ , and section stall ($3/4$ chord) angle of attack α_s are reduced not only to lower the profile drag but more to deliberately prompt stall at high T and constant Ω near the tip [7]. The constant rpm means such more tangent tips are safe in overinducing in lighter, much less powerful winds below design. But part of the remarkable success of large Hawts is due to the broadness of a near robust optimum in mid-blade, and robust design is even more relevant to small Hawts.

6 ASYMPTOTICALLY OPTIMAL TWO-DIMENSIONAL VAWT AND ROBUST VAWT BLADE ELEMENTS

Appendix 2 shows the normal interference as $m \rightarrow 0$ is a , half the normal velocity change $2a$ for any θ so equation (5) holds $dP/ds \rightarrow 2\rho(1 - a)^2 a(T \sin \theta)^3$. Were the Vawt blades to follow a semicircular path across the wind, and then return completely feathered, integrating over θ and normalizing by the undisturbed wind energy flux gives $C_p = P/\rho r T^3$ only $32/81 = 0.39$ at optimum $a = 1/3$. Since this is $2/3$ of the ideal Hawt, a contribution from the return pass is desirable.

The Hawt crosswind flows at the rotor neatly separate into azimuthal thrust reaction with little or no

regain and the implicit expansion radial flows which are regained at the end of the expansion. In the double pass Vawt, the expansion must be considered explicitly and the thrust reaction flows from the windward tangential velocity jump at the actuator cylinder are opposed by the leeward's.

Figure 3 considers stream tubes in a complete two-dimensional Vawt by taking the velocity of approach to the leeward crossing at azimuth ϕ as the full windward wake velocity Γ , which as $m \downarrow 0$ is reduced by fraction $2a$ in its radial component from T . Conversely, the vortex wake of the leeward pass would induce negligible flow at the windward crossing, so the lee interference immediately optimizes at $1/3$. As $m \downarrow 0$ there is mirror symmetry about the wind diameter $\theta = \phi = 0$. Γ 's key leeward radial (normal) component is $\ni T$

$$\ni = \frac{\Gamma \sin(\phi + \psi)}{T} \rightarrow \cos \theta \sin(\theta + \phi) - (1 - 2a) \sin \theta \cos(\theta + \phi) \quad (20)$$

showing at small $\theta + \phi$ the downwind crossing normal component is decreased by any remnant of the upwind one. Therefore, it pays for the upwind side passes to

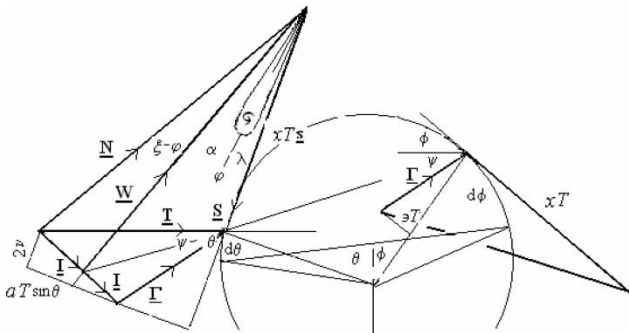


Fig. 3 Optimum Vawt

have the maximum sensible $a = 1/2$ to remove all of the upwind radial component. However, there will be some leeward tangential resolution of the windward tangential component of T that will be unrecoverable, until $\theta + \phi = \pi/2$.

Then the two radial components are independent and complete so for this stream tube a should be $1/3$ for the windward crossing as well. Its final wake velocity is $T/3$, after the outwards jog expanding through the rotor.

dQ , the incremental volume flux/ Tr , and the coefficient of performance C_p satisfy

$$dQ = \frac{2 \ni d\phi}{3} = (1 - a) \sin \theta d\theta \quad (21)$$

$$\frac{dC_p}{dQ} \rightarrow \frac{2a(1 - a) \sin^2 \theta + 4 \ni^2}{9} \quad (22)$$

The optimum recovery of wind energy from the centre stream tubes is at no windward interference $a = 0$, with the leeward width then $3/2$ the original and windward width. With the sum of the widths limited by the ultimate closure of the circle, the stream tube expansion is best delayed to the leeward pass. The above explain the manually optimized a in Fig. 4 from spreadsheet integration of the above equations out from the centre-line until $\theta = -\phi \approx 0.14 \approx 8^\circ$. The net C_p approaches the Hawt $16/27$ as $\Delta\theta \downarrow 0$. Nearly, $2/3$ of the power again is captured in the leeward pass, the loss by shadowing at intermediate ϕ being compensated by the enhanced recovery at small ϕ ; but now with roughly matching windward captures for the matching θ . The rotor downwind induced drag coefficient $C_T = E/\rho r T^2$ integrates to 0.82 versus $8/9$, for a Hawt, so the efficiency $\eta = C_p/C_T = 0.71$ versus $2/3$ for better ideal array capture. However the profile drag C_p tends to $2\pi C_D x^3$, π times the Hawt correction due to the circumferential path being π greater than the diameter swept but for the same design x and mean α ,

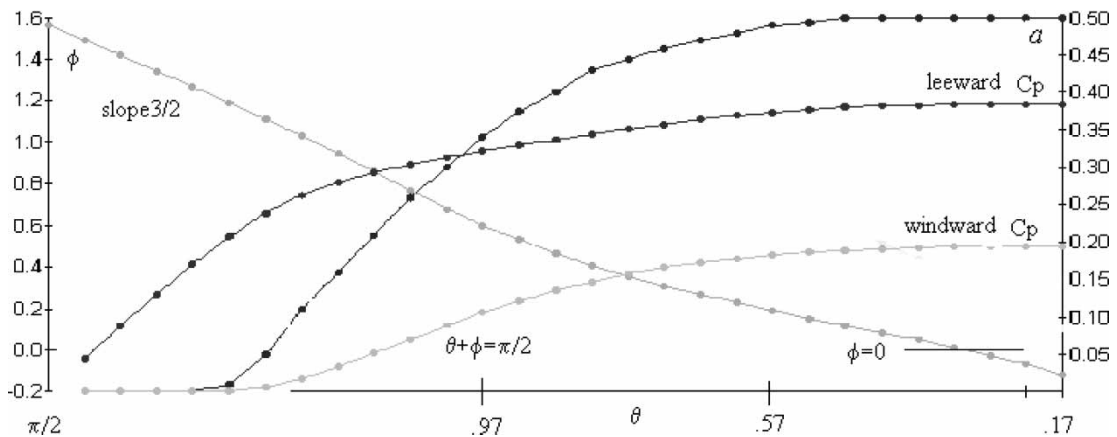


Fig. 4 Lee azimuth, windward interference and integrated powers versus windward azimuth

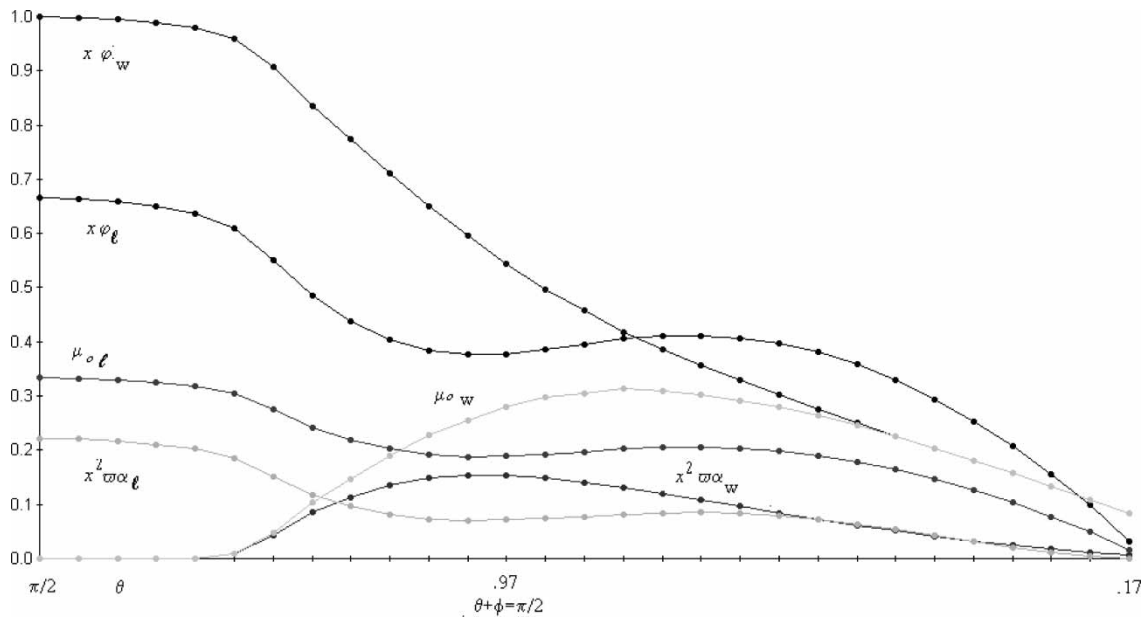


Fig. 5 Windward and lee blade angles and flow versus windward azimuth

the Vawt ϖ is smaller by 0.14/0.22 or 0.63 for twice the drag C_p .

Figure 5 plots the apparent wind angles as $x\varphi$, and uses equation (16) to plot the angles of attack as $x^2\varpi\alpha$. However, the constant $\varpi = Bc/4r$ cannot vary, as ξ_d and φ_d do, with θ for this Vawt optimum to be everywhere stationary (robust) with x . Whereas a Hawt blade's pitch cannot be controlled to remain exactly optimal with x because then its twist would have to vary, but can be robustly near optimal at fixed pitch and twist.

Also plotted is the asymptotic induction $\mu_0 = \varpi x \sin \alpha / \sin \varphi$ which is a constant ϖx in θ for tangent blades. The peak lateral velocity is $0.46T$ for the windward wake at small θ , and $0.19T$ at $\theta = 1.27$ in the lee wake. The former is indicative of the error in the induced flow at the rotor of methods ignoring lateral velocities and half the latter or 10 per cent, the residual error here.

Dynamically pitching the blades by a balance of pitch torque as $W^2\alpha$ and quadratic torque as $\Omega^2\lambda^2$ from a mass restrained centrifugally by a blade cam would make α diminish asymptotically as $(\varphi - \alpha)^2$ and so ultimately as φ^2 , varying as the required m^2 . On the lee-ward pass by equation (16) this could give the required $a = 1/3$, but not the optimal windward a variation with θ . A dynamic pitch system can allow the blades to feather when braked in high wind and vulnerable without their centrifugal preload. A computer pitching and measurement system [8] would be capable of generating any $\alpha(\theta, x)$ and definitively optimizing it. The clockwise moment M is $-1/8\pi\rho Wc^3\Omega d\alpha/d\theta$ for pitching about the 1/4 chord balance point. The pitch damping power/blade is the product with the

blade pitch velocity $-M\Omega d\lambda/d\theta$ with mean $\Delta C_p \rightarrow B(c/r)^2 \Sigma \Delta(\omega x^2 \alpha) \Delta(x\varphi) / 2\Delta\theta$. This sum bottoms at $-0.092B(c/r)^2$ in the optimal windward pass before climbing to a net damping residue of $0.033B(c/r)^2$. Thus energy conservation would be desirable in the control system. This is inherent in a mechanical articulation such as a cam track, but the Giromill [8] did not recover positive pitch motor power and sought an extreme square wave in α for a significant net pitch power penalty. That strategy was only sensible for α limited by stall; otherwise, after only nominal testing, the Giromill blades were held tangential, ignoring McDonnell's own theory [8] which agreed that α should vanish as m^2 . In any case, a golden opportunity to definitively optimize Vawt blade pitching for performance at each x at near full scale was tragically lost.

Generally, Vawt designs have been preoccupied with stall, and have not addressed the other source of low induction (interference) at small x and the complementary non-benign over-induction at high x (also compromised by the large drag penalty of the side zones and struts). These imbalances of I/T stem from the simplest fixed tangent blades being as far from robustly pitched as conceivable. Thus even without stall and drag, tangent Vawt C_p peaks would still be quadratically much narrower in x than closer-to-robustly-quartically-optimal Hawts and so still less successful at constant Ω synchronous generation in the windspeed spectrum. Whereas the tidal current spectrum is much narrower with a definite and low maximum velocity so stall of a fixed blade and rpm Vawt can be avoided (except as it is started from the grid).

A (non-optimal) Vawt design could be robust, i.e. have stationary interferences $a(\theta)$, and be benign, if at small angle and m equation (16) $\varpi(\varphi - \lambda(\theta)) = (\xi - \varphi)\varphi$ were invariant to small changes in $\xi(\theta)$, with φ proportional as $(1 - a)\xi$. This requires $\alpha = \lambda(\theta) = \varphi_d/2$ still and constant $\varpi = 2(\xi_d - \varphi_d)$. These are, respectively, half and twice the tangent Vawt values $\alpha = \varphi$, and constant $\varpi = \xi_d - \varphi_d$, so its narrow C_P peak and over-inducing at high x can be remedied by doubling the solidity and making the blades follow a wind-oriented cam to bisect its φ_d at its best (design) x_d (at the price of doubling the drag penalty). The above windward/leeward BEM picture and various corrections and the cam shape are analysed for the tangent Vawt in a separate paper which finds its peak C_P to be 0.53 [9].

7 CONCLUSION

The standard momentum theory has been exactly optimized for the windpower captured by blades moving at any velocity relative to the true wind. The best Vawt pitch cycles $\lambda(\theta, x)$ reach the Betz limit. To make the optimum robust with only quartic losses for small changes in the wind, and the loading benign for bigger changes just requires the Hawt blade to be fixed at 1/3 the nominal design wind angle or the Vawt to follow a 10 per cent suboptimal robust cam $\lambda(\theta)$ pitch cycle. Robust design as based on quasisteady BEM seems most applicable to small off-grid windmills where it also avoids the high unproductive fatigue loads of the turbulent over-induced state in high winds.

Besides the simple understanding of the Hawt success attained, the possibilities of always optimal pitch $\lambda(\theta, x)$ or robust and benign cyclic pitch $\lambda(\theta)$ might help resurrect the Vawt, especially as so articulating Vawt blades is easier to structurally engineer than on a Hawt, where the fixed pitch optimum is twisted and already robust, quartic, and benign anyways.

ACKNOWLEDGEMENTS

Thanks to Professors Rob East of Southampton and Doug Greenwell of City University for checking many equations and to the referees.

REFERENCES

- 1 **Glauert, H.** Windmills and fans. In *Aerodynamic theory* (Ed. W. F. Durand), 3L-XI, 1935, pp. 324–331 (J. Springer, Berlin) (reprinted by Dover Publications New York, 1963, TL 570 D865).

- 2 **Stewart, H. J.** Dual optimum aerodynamic design for a windmill. *AIAA J.*, 1976, **14**(11), pp. 1524–1527.
- 3 **Maalawi, K.** and **Badawy, M.** A direct method for evaluating performance of horizontal axis wind turbines. *Renew. Sustain. Energy Rev.*, 2001, **5**, 175–190
- 4 **Eggleston, D. M.** and **Stoddard, F. S.** *Wind turbine engineering*, 1987 (Van Nostrand, New York).
- 5 **Farthing, S. P.** Optimal Hawt with swirl expansion decay, submitted 25/05/07 to *Wind Energy*: WE-07-0042, available from www.econologica.com/WE-07-0042.pdf.
- 6 **Farthing, S. P.** Robustly optimal fixed pitch Hawt with tip correction and drag. Submitted 28/9/07 to *AIAA J.*, available from www.econologica.com/30455.pdf.
- 7 **Hansen, A. C.** and **Butterfield, C. P.** Windmill aerodynamics. *Annu. Rev. Fluid Mech.*, 1993, **25**, 115–149.
- 8 **Brulle, R.** McDonnell Aircraft 40 kw Giromill Phase II, RFP-3304, Subcontract No, PF- 64100 to Rockwell International, US DOE, 1980, pp. 1–62.
- 9 **Farthing, S. P.** VAWT vector streamtube theory. Available from www.econologica.com/vp.pdf.
- 10 **Glauert, H.** Induced velocity in blade element theory. In *Aerodynamic theory* (Ed. W. F. Durand), 3L-V-5, 1935, pp. 220–222 (J. Springer, Berlin) (reprinted by Dover Publications New York, 1963, TL 570 D865).
- 11 **Batchelor, G. K.** *Introduction to fluid dynamics*, exercise 5.3, 1967 (Cambridge University Press).

APPENDIX 1

Notation

a'	the tangential interference factor $v/xT \sin \theta$
a	the normal (radial) interference factor $(\mu/T \sin \theta)$
B	the number of blades
c	the local blade chord
C_T	thrust coefficient = $2/\rho T^2/E$ swept area
C_D	sectional profile drag coefficient
C_P	rotor coefficient of power/undisturbed kinetic energy flux through the swept area $2P/\rho T^3/\text{swept area coefficient}$
E	downwind force, actuator induced drag
I	the induction, half the velocity change the blades produce downstream in their wake
k	reduced frequency based on chord $\Omega c/T$
\mathbf{k}	unit vector along the blade span
L	aerofoil lift vector
m	inverse speed ratio $T/\Omega r = 1/x$
M	the clockwise pitch damping moment about the 1/4 chord point
\mathbf{n}	unit vector normal to the path directed downwind

N	the no-lift or nominal apparent wind $T - S$
P	the dimensional power per unit length of span
Q	non-dimensional streamtube volume flux/ Tr per unit span
r	the radius from the blade element to the axis of rotation
s	circumferential distance along the blade path
\mathbf{s}	unit vector in the direction of instantaneous blade movement
\mathbf{S}	the blade velocity vector
T	windspeed
T_d	design windspeed of peak wind-power density
\mathbf{T}	true undisturbed wind vector
W	speed or magnitude of the apparent wind
\mathbf{W}	net apparent wind vector $\mathbf{T} - \mathbf{S} + \mathbf{I}$
x	local speed ratio $\Omega r/T$
X	the Hawt tip speed ratio

α	3/4 chord angle of attack to \mathbf{W}
α_s	the (dynamic) stall onset value of α
prefix δ	a small variation
Δ	a small numerical increment
η	Glauert thrust efficiency C_p/C_T
θ	the true wind angle to the blade path
κ	one third of the design value of ξ , $\kappa = \xi_d/3$
λ	the blade pitch or angle of the 3/4 chord centreline to the blade path
μ	normal component of \mathbf{I} upwind
$\mu_0 = xI/W$	representative of the non-dimensional induction I/T at high x
ξ	the nominal or no-lift apparent wind N angle to the blade path
$\xi_{1/2}$	the value at which a peaks at 1/2
ρ	fluid density
σ	true local solidity = blade chords/circumference of blade travel $Bc/2\pi r$
v	antitangential (negative θ direction) component of \mathbf{I}
ϕ	Vawt downstream azimuthal angle (θ without streamtube expansion)
φ	the true or complete apparent wind \mathbf{W} angle to the blade path
ψ	the angle of the wake wind to the true wind
$\bar{w} = Bc/4r$	half the net blade chord divided by the diameter $\pi\sigma/2$

Ω	angular velocity of rotation in radians per unit time
\ni	leeward downwind radial component of $\mathbf{\Gamma}/T$
$\mathbf{\Gamma}$	the wake velocity $T - 2I$
\downarrow	tends down to from greater than (above)
\uparrow	tends up to from less than (below)

Subscripts

d	design value
l	Vawt leeward pass
w	Vawt windward pass

APPENDIX 2

The induced velocity at Hawts and Vawts

Just in front of a Hawt, irrotationality and symmetry require the tangential velocity induced by even an expanding vortex wake to exactly cancel that induced by the bound vorticity of the actuator disc. Since this bound vortex sheet induces equally and oppositely on its two sides, if the tangential velocity increase across the disc is $2v$, the tangential component of $2I$, the tangential velocity induced by the wake alone on the disc must be v [10]. (For a general actuator asymmetric about the wind direction there must be a similar tangential jump across the bound vortex sheet, but from a possible tangential component of induced velocity just in front.)

If the circumferential Hawt wake vorticity is considered an unexpanded semi-infinite tube behind the disc, then by symmetry its axial induction is also half its induction deep inside the wake where the tube appears infinite [10].

A separate paper [5] considers in detail the BEM ignoring the expansion of v , and its centrifugal pressure terms in the axial balance for a Hawt and finds it to imply that the maximum velocity change components are dissipated ultimately in the wake. If the swirling flow behind the rotor is stable enough to expand ideally (before viscously dissipating), some of the kinetic energy of its tangential swirl velocity v component is converted into pressure regain, and the BEM theory here is found to (under) predict C_p by at most 3.5 per cent.

When the BEM Hawt loses flow symmetry by yawing or for a Vawt, there should still be no net pressure (work) on the streamtube end sections, so (in the earth frame) the transfer of wind kinetic energy to the

actuator is

$$\begin{aligned}\frac{dP}{ds} &= \frac{1}{2}\rho(\mathbf{W} \cdot \mathbf{n})[\mathbf{T} \cdot \mathbf{T} - (\mathbf{T} + 2\mathbf{I}) \cdot (\mathbf{T} + 2\mathbf{I})] \\ &= -2\rho(\mathbf{W} \cdot \mathbf{n})\mathbf{I} \cdot (\mathbf{T} + \mathbf{I}) \\ &= \frac{d\mathbf{L} \cdot \mathbf{T}}{ds} - \frac{1}{2}\rho(\mathbf{W} \cdot \mathbf{n})(2\mathbf{I})^2\end{aligned}\quad (23)$$

(The latter expresses the view from the wind frame that the useful actuator power dP/ds is the difference between the total work done by the wind, T times the actuator induced drag dE , and the wasted power flux of the dissipated kinetic energies of the velocity change.)

Now if \mathbf{F} is the flow over the ground at the actuator, then $\mathbf{W} = \mathbf{F} - \mathbf{S}$ so $d\mathbf{L} \cdot \mathbf{W} = 0$ means $\mathbf{I} \cdot \mathbf{S} = \mathbf{I} \cdot \mathbf{F}$ so the power per unit area is $dP/ds = d\mathbf{L} \cdot \mathbf{S}/ds = -2\rho(\mathbf{W} \cdot \mathbf{n})\mathbf{I} \cdot \mathbf{S} = -2\rho(\mathbf{W} \cdot \mathbf{n})\mathbf{I} \cdot \mathbf{F}$. Equating to the middle term above gives $\mathbf{I} \cdot (\mathbf{F} - \mathbf{T} - \mathbf{I}) = 0$. Thus the real induced flow at the actuator $\mathbf{J} = \mathbf{F} - \mathbf{T}$ differs from

\mathbf{I} only perpendicular to \mathbf{I} , either insignificantly span-wise (k) (implicitly in the Hawt) or in the direction of \mathbf{W} . Thus $\mathbf{J}-\mathbf{I}$ changes the magnitude W of the apparent wind but not its direction φ . This is almost even true when the swirl expands [5]. Since the norm of $\mathbf{J}-\mathbf{I}$ should be less than $I/2$ or $T/6$ and $W \downarrow xT$ any effect is negligible for say $x > 2$. That generalizes Glauert's kinetic energy flux argument for $\mathbf{J} \cdot \mathbf{T} = \mathbf{I} \cdot \mathbf{T}$ in his one-dimensional Hawt limit of high x to any windmill at high x .

The case of blades translating across the wind is cautionary. Without a closed path there is no completion of a vortex cylinder to separate undisturbed stream-flow from an internal slower, but ambient pressure, wake like that of a bluff body. Any net lift force implies a net transverse velocity in the wake which is likewise incompatible with a cylindrical wake in undisturbed flow. Far downstream of a body with lift Batchelor [11] gives the lift perturbing the stream flow outside the diffusive wake zone to the order of the inverse of lateral distance squared.

